Validation of Slosh Modeling Approach Using STAR-CCM+

David J Benson[(1)], Wanyi Ng[(1)]

[(1)]National Aeronautics and Space Administration (NASA) Goddard Space Flight Center, 8800 Greenbelt Rd, Greenbelt, Maryland, 21076, United States of America

KEYWORDS: slosh, CFD, computational fluid dynamics, PMD, propellant management device

Abstract:

Without an adequate understanding of propellant slosh, the spacecraft attitude control system may be inadequate to control the spacecraft or there may be an unexpected loss of science observation time due to higher slosh settling times.

Computational fluid dynamics (CFD) is used to model propellant slosh. STAR-CCM+ is a commercially available CFD code. This paper seeks to validate the CFD modeling approach via a comparison between STAR-CCM+ liquid slosh modeling results and experimental, empirically, and analytically derived results. The geometries examined are a bare right cylinder tank and a right cylinder with a single ring baffle.

1. INTRODUCTION

Propellant slosh is the movement of liquid propellant within a propellant tank. Propellant slosh is excited by thrusters, momentum wheels, launch vehicle motion, spacecraft separation from launch vehicle, and deployments. When firing thrusters for a sustained time, the propellant will settle in the opposite direction to the acceleration of the spacecraft. This settling event results in a periodic motion as the propellant slosh motion dampens out.

Because propellant slosh exerts forces and torques on the spacecraft, propellant slosh can disturb the spacecraft pointing, and in extreme cases propellant slosh can result in a spacecraft tumbling out of control. Even when propellant slosh is controlled, excessive propellant slosh can reduce the amount of observing time for science instruments. Due to the potential for negative effects on the spacecraft and its mission, it is important to predict the magnitude, frequency, and damping of the propellant slosh.

Once computational fluid dynamics (CFD) has been used to model the propellant, equivalent mechanical models can be derived that can approximately model the slosh magnitude, frequency, and damping [1]. These equivalent mechanical models are used in Monte-Carlo type simulations for attitude control system validation, instead of CFD, due to the computational expense of running full CFD models.

The CFD model outputs center of mass location of the propellant, forces on the tank, torques on the tank, and images of the volume fraction. The pressurant gas is included in the center of mass calculation, but due to the gas having a much lower density, its influence is negligible. This data can be used to determine the sloshing frequency, damping ratio, sloshing mass, sloshing mass location, static mass, and static mass location, which are parameters in the equivalent mechanical sloshing model. Eq. 1 [2] describes a pendulum equivalent mechanical sloshing model. A similar equation can be derived for a spring-mass-damper system, if preferred. θ_0 is the pendulum initial offset angle, $\theta(t)$ is pendulum angular position as a function of time, ζ is the damping ratio, t is time in seconds, and ω is angular frequency.

$$\theta(t) = \theta_0 e^{-\zeta\omega t}\left(\frac{\zeta\omega}{\omega\sqrt{1-\zeta}}\sin\left(\omega\sqrt{1-\zeta^2}\,t\right) + \cos\left(\omega\sqrt{1-\zeta^2}\,t\right)\right) \quad (1)$$

In some cases, multiple sloshing masses are necessary to capture multiple slosh frequencies. The accuracy of the equivalent mechanical sloshing model depends on the accuracy of the CFD model.

STAR-CCM+ is a commercially available CFD software package that has been used to model slosh [2, 3, 4, 5]. Dodge and Benson et al [1, 2, 3] show how CFD slosh data has been used to derive pendulum parameters for flight missions.

STAR-CCM+ uses a body centered mesh with the ability to refine the mesh near the solid surfaces and within specific user defined volumes. For this work, both polyhedral and trimmed three-dimensional meshes are used. The liquid and gas phases are modeled using a volume of fluid (VOF) method. A settling acceleration is applied using a gravity model.

Experimental results, empirical relations, and analytic equations for slosh in simple shaped containers are available in literature [1]. The results from STAR-CCM+ models are compared to frequency and damping derived from experimental results, empirical relations, and analytic equations for a bare right circular cylinder tank and a right circular cylinder tank with a single baffle. By comparing STAR-CCM+ results with the experimental, empirical, and analytic results for both a bare tank and a tank with a single baffle, the STAR-CCM+ modeling approaches can be validated for bare tanks and validation can be implied for tanks with internal structure. This approach to validating CFD codes has been followed previously [4, 6, 7].

2. RESULTS AND DISCUSSION

2.1 Bare tank case

2.1.1 Model description

One of the simplest tank shapes that can be studied for slosh is the right circular cylinder. Many flight tanks are right circular cylinders with hemispherical caps. The tank studied for this paper is shown in Fig. 1. The tank size is chosen because it approximates the size of many large propellant tank used for in-space propulsion.

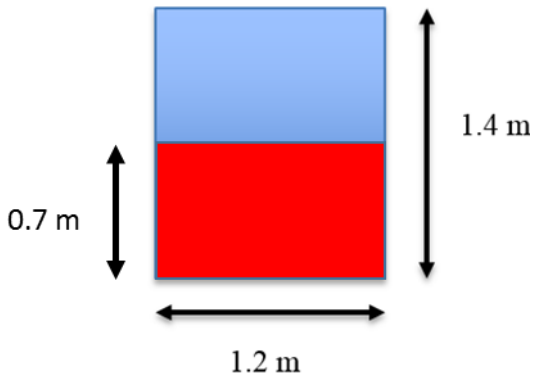

Figure 1. Right circular cylinder bare tank

Tab. 1 shows the mesh types, cell count (higher cell count corresponds to smaller average cell size), and settling acceleration for the models studied. To restrict the number of independent variables, the time step is not varied for meshes with the smallest cell sizes. Not varying the time step still gives valid results because an implicit solver is used, though it is noted that improved results may be possible if the time step is decreased for finer meshes.

Table 1. Bare tank model cell size, cell count, and settling acceleration

Mesh Type	Approximate Cell Count	Settling Acceleration (m/s^2)
Polyhedral	305k	0.0200
Polyhedral	305k	0.0981
Polyhedral	557k	0.0981
Polyhedral (volumetric control)	1110k	0.0981
Trim (volumetric control)	327k	0.0981
Trim (volumetric control)	618k	0.0981
Trim (volumetric control)	1190k	0.0981

A polyhedral mesh is used by National Aeronautics and Space Administration's (NASA) Goddard Space Flight Center (GSFC) to model slosh because this mesh type typically has fewer cells than a tetrahedral mesh and the orientation of the mesh is random. Because the cell orientation is random, it can give accurate results for flow in many different directions. The polyhedral mesher within STAR-CCM+ optimizes the number of polyhedral cells, as well as the number of sides for each cell, based on user inputs. The STAR-CCM+ polyhedral mesh's polyhedral cells have an average of 14 cell faces [8]. A trim mesh was also used. A trim mesh is made up of cubes that are trimmed off at solid interfaces. A trim mesh may have lower dissipation than a polyhedral mesh, which affects the damping. Both the polyhedral and the trim mesh were used with the prism layer mesher. The prism layer mesher constructs smaller cells near the solid surfaces to better catch boundary layer effects and then grows the cell size as the cells get further away from the wall so that there is a smooth transition to the core mesh. In some models, a volumetric control is used to refine the cell size near the liquid-gas interface. The volumetric controls were added later in the modeling process, which is why the first polyhedral cases do not have it.

Fig. 2 and Fig. 3 show cross sections of the densest polyhedral and trim meshes.

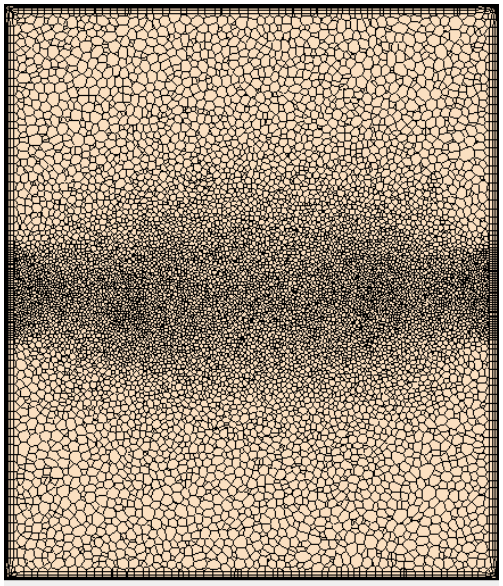

Figure 2. Polyhedral mesh with approximately 1110k cells

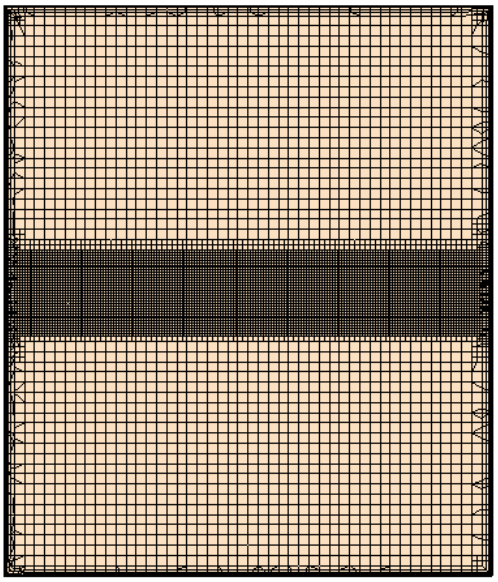

Figure 3. Trim mesh with approximately 1190k cells

The model was initialized with the liquid filled to 50% of the tank volume and the liquid offset to one side, as shown in Fig. 4. The liquid-gas interface makes a 3 degree angle with the horizontal plane.

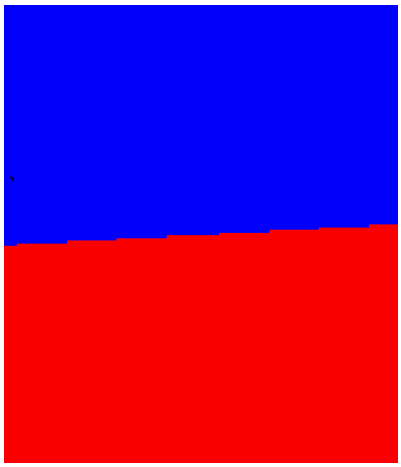

Figure 4. Model initial liquid position (bottom section is liquid)

The liquid in the model is nitrogen tetroxide (NTO), which is a common oxidizer used in spacecraft propulsion systems. The pressurant gas is nitrogen, though the results would be the same if a gas like helium was used.

The model run times varies with the mesh density and type. Using 16 cores, the models with the roughest meshes would take less than 1 day of wall clock time to model 150 seconds of slosh. Using 100 cores, the models with the finest meshes took several days of wall clock time to model 150 seconds. The models with trim meshes had a harder time converging. Since it took longer to converge within each time step, the total modeling time was larger than the models with a polyhedral mesh for models with a similar number of cells.

2.1.2 CFD results and discussion

Fig. 5 and Fig. 6 show plots of the center of mass of the liquid and force exerted on the wall outputs for the first 75 seconds of slosh. At least 150 seconds of slosh are modeled and used when determining the frequency and damping, but the results in Fig. 5 and Fig. 6 are truncated to 75 seconds to better show the differences between the different models. The torque outputs are similar to those of the forces and are not included in the paper.

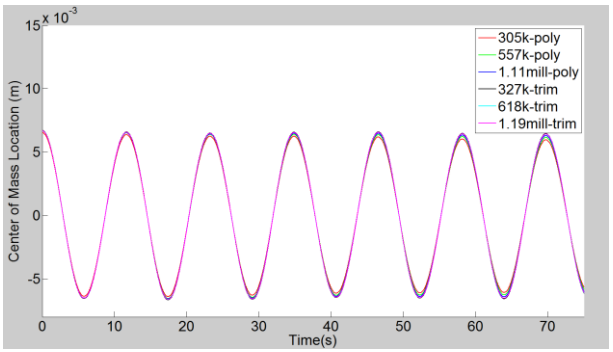

Figure 5. Center of mass movement for bare tank models

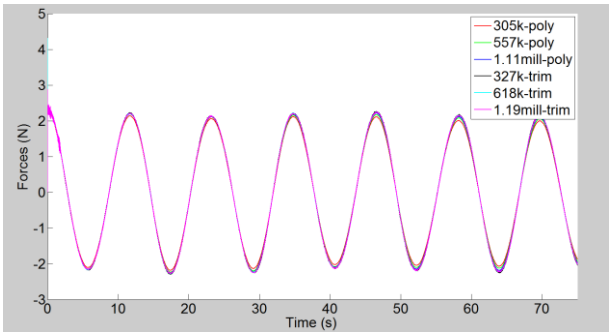

Figure 6. Forces on tank wall of bare tank models

Fig. 5 -9 show that the magnitude and the frequency of both the center of mass movement and the forces on the tank between the different models are very similar at the beginning of the model run, but diverge as the effects of damping accumulate. The models with the polyhedral mesh have a higher damping than the models with the trim mesh, but the trim mesh models also have more noise, as shown more clearly in Fig. 7-9.

The noise shown in Fig. 7-9 can be explained by the trim model struggling to converge within each time step. Because the solver uses a maximum number of inner iterations for each time step, it is possible to march forward in time even if the model has not converged within the time step once the maximum number of inner iterations is reached. Also, when a volumetric mesh refinement is used, there is more noise in the data. The noise could be caused by a time step that is too large or perhaps difficulty in the solution converging near the transition between the finer mesh regions and the rougher mesh regions.

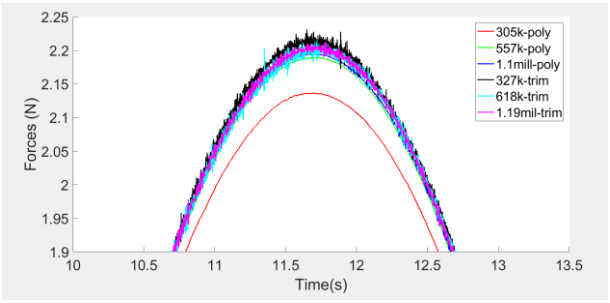

Figure 7. Forces on tank wall around 11.5 seconds (2nd peak)

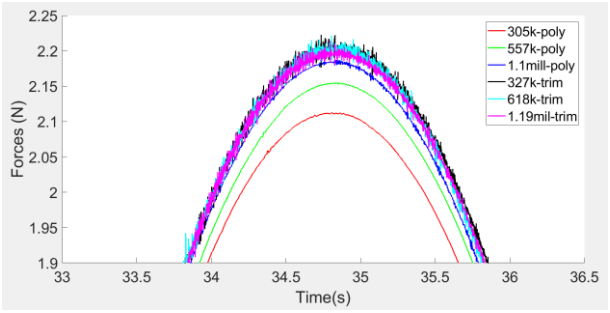

Figure 8. Forces on tank wall around 34.75 seconds (4th peak)

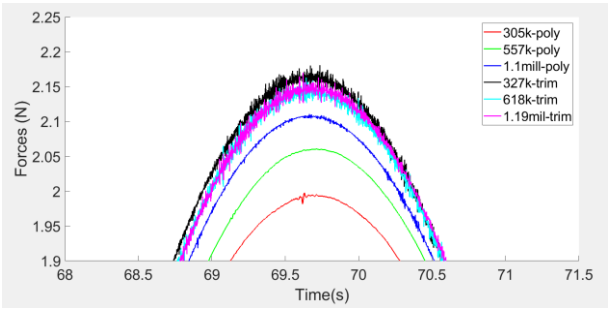

Figure 9. Forces on tank wall around 69.5 seconds (6th peak)

The volume fraction output shows a well-defined liquid-gas interface, as shown in Fig. 10 and Fig. 11. However, the polyhedral mesh gives a more diffuse liquid-gas interface, in part because no volumetric mesh refinement is used around the gas liquid interface at the roughest mesh refinement. A less defined liquid-gas interface may contribute to the greater variability in results between the models with polyhedral meshes.

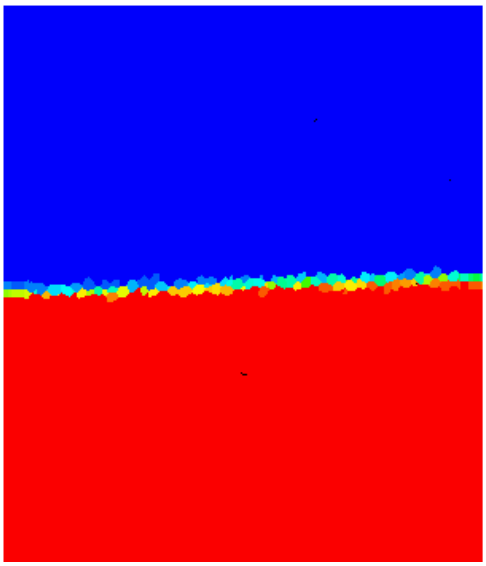

Figure 10. 305k cell polyhedral mesh liquid volume fraction (bottom section is liquid)

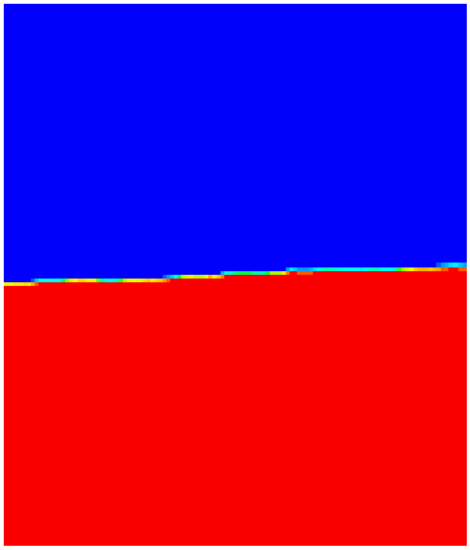

Figure 11. 327k cell trim mesh liquid volume fraction (bottom section is liquid)

2.1.3 Post-processed CFD results and discussion

The center of mass movement output from the CFD models is used to derive the frequency and damping ratio of the slosh. The force or torque outputs could be used, but because these results contain more noise than the center of mass movement output, the center of mass movement results are used.

The frequency is computed from the CFD results by calculating the time between each peak and then averaging these periods to get an average period for the entire run. The period is then inverted to give the frequency in Hertz (Hz).

From the geometry, an equivalent mechanical model pendulum length can be calculated using Eq. 2 [1], and once the length of the pendulum and the settling acceleration is known, Eq. 3 [1] can be used to calculate the expected frequency in Hz. L is the pendulum length, R is the radius of the cylinder, h is the fill height, g is the settling acceleration (see Table 1), and f is the frequency in Hz.

$$L = \frac{R}{1.841 \tanh(1.841\, h/R)} \qquad (2)$$

$$f = \frac{1}{2\pi}\sqrt{\frac{g}{L}} \qquad (3)$$

Tab. 2 shows a comparison between the frequencies calculated from the CFD results and the equivalent mechanical model predicted frequencies.

Table 2. Bare tank frequency comparison

Mesh Type	Cell Count	Simulated Frequency (Hz)	Predicted Frequency (Hz)
Poly	305k	0.0388	0.0389
Poly	305k	0.0860	0.0861
Poly	557k	0.0860	0.0861
Poly	1110k	0.0860	0.0861
Trim	327k	0.0860	0.0861
Trim	618k	0.0860	0.0861
Trim	1190k	0.0860	0.0861

The results show that all of the mesh types result in good predictions of the sloshing frequency, as compared to the predicted equivalent mechanical model frequency. The difference between the CFD frequency and the predicted frequency for the models that use an acceleration of 0.0981 m/s^2 is 0.1% and the difference for the model that uses an acceleration of 0.02 m/s^2 is 0.3%.

The damping is computed by fitting an exponential curve to the positive peaks and negative peaks, as shown in Fig. 12 and Fig. 13. The fitting is accomplished using Matlab's Curve Fitting toolbox. The positive peaks are called peaks and the negative peaks are called valleys. Fig. 12 and Fig. 13 show the fit for the 557k polyhedral mesh model results, but all the other models give results that have similar trends.

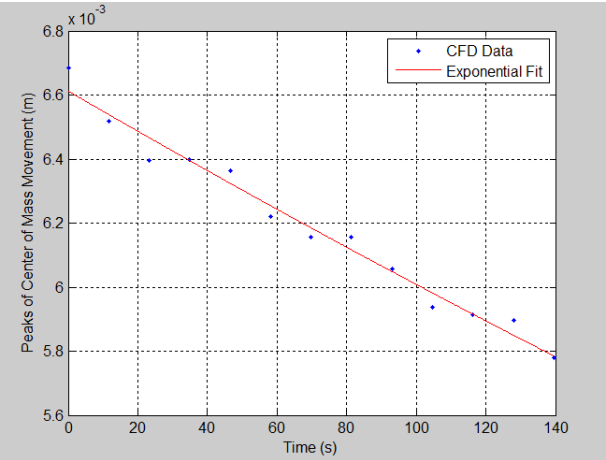

Figure 12. Exponential fit to center of mass movement peaks

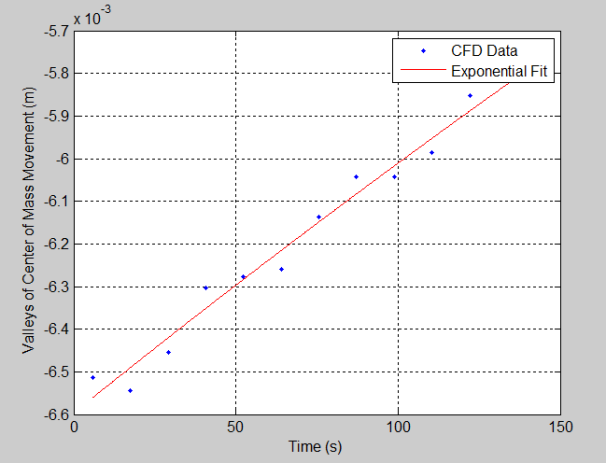

Figure 13. Exponential fit to center of mass movement valleys

An exponential fit can predict the general damping of the slosh, but Fig. 12 and Fig. 13 show that there is more than one sloshing mode present. This work does not attempt to quantify the other sloshing modes. The other sloshing modes add complexity when deriving equivalent mechanical models, but do not add much fidelity due to their small influence on the bulk motion of the liquid. Reference [1] gives a thorough discussion on the presence of other sloshing modes in bare tank slosh.

Eq. 5 [1] was proposed by Mikishev and Dorozhkin for predicting the damping of slosh in a bare right cylindrical tank. Re_1 is the Reynolds Number, v is the kinematic viscosity of the sloshing liquid, g is the settling acceleration, ζ is the damping ratio, h is the liquid fill height of the tank, and R is the radius of the tank.

$$Re_1 = \frac{v}{\sqrt{gR^3}} \tag{4}$$

$$\zeta = 0.79\sqrt{Re_1}\left[1+\frac{0.318}{\sinh\left(1.84\frac{h}{R}\right)}\left(1+\frac{1-\frac{h}{R}}{\cosh\left(1.84\frac{h}{R}\right)}\right)\right] \tag{5}$$

Eq. 6 [1] was proposed by Stephens [1] to calculate damping of slosh in a bare right cylindrical tank. Both Eq. 5 and Eq. 6 use Eq. 4 [1] to calculate the Reynolds Number.

$$\zeta = 0.83\sqrt{Re_1}\left[\tanh\left(1.84\frac{h}{R}\right)\left(1+2\frac{1-\frac{h}{R}}{\cosh\left(3.68\frac{h}{R}\right)}\right)\right] \tag{6}$$

Eq. 5 and Eq. 6 are the empirical correlations used to calculate the expected damping for comparison with the CFD damping. The CFD damping calculated in Eq. 7. Eq. 7 comes from the exponential term in Eq. 1 with ω being replaced by 2πf. E_{fit} is the damping coefficient from the exponential fit to the CFD results and f is the frequency of the slosh as derived from the CFD results.

$$\zeta = \frac{E_{fit}}{2\pi f} \tag{7}$$

Eq. 7 is needed to account for the fact that a higher frequency will result in the slosh damping out more quickly.

Tab. 3 compares the CFD damping from Eq. 7 and the predicted damping from Eq. 5 and Eq. 6.

Table 3. Bare tank damping comparison

Cell Count	Exp Damping Peaks (%)	Exp Damping Valley (%)	Empirical Damping Eq. 5 (%)	Empirical Damping Eq. 6 (%)
305k	0.2689	0.2295	0.1817	0.1599
305k	0.2087	0.2042	0.1221	0.1074
557k	0.1773	0.1722	0.1221	0.1074
1110k	0.1052	0.1058	0.1221	0.1074
327k	0.0513	0.0484	0.1221	0.1074
618k	0.0568	0.0573	0.1221	0.1074
1190k	0.059	0.0521	0.1221	0.1074

The results in Tab. 3 show that the models with the polyhedral mesh over-predict the damping for rougher meshes, but as the mesh cell count increases, the results match the expected damping, as predicted by Eq. 6, very well. The models with the trim mesh significantly under-predict the

damping, even as the cell count is increased. When the exponential damping from the peak data is averaged with the exponential damping from the valley data, the model results with the finest polyhedral mesh give a damping that differs from the Eq. 5 damping by 1.7% and the Eq. 6 damping by 0.2%. The model results with the roughest polyhedral mesh give a damping that differs from Eq. 5 damping by 8.4% and Eq. 6 damping by 9.9%. A fine polyhedral mesh should be used to get the best damping, but the user may opt to accept the higher error if the model run time is too long with the finest mesh.

The results validate the approach taken to use STAR-CCM+ to model slosh in a bare tank because the difference between the CFD derived frequency and the predicted frequency using equation from [1] differ by only 0.1% and the CFD derived damping and the predicted damping using equations from [1] differ by 1.7% and 0.2%.

2.2 Baffled Tank Case

2.2.1 Model Description

Propellant tanks usually contain a propellant management device (PMD). While PMDs add more complexity to the slosh than just a simple baffle [1], in the absence of experimental data from PMD flight tests, CFD validation to a single baffle case can indicate that the CFD modeling approach is appropriate. The author acknowledges that data from a flight-like PMD would be preferable over that of a single ring baffle, but since each PMD design is different, unless the model was compared against test data for a similar PMD design every time, even validation against PMD test data does not prove that the CFD modeling approach would work for all PMD designs. A similar approach is used by other authors [6,7].

Experimental and analytic results exist for a ring baffled tank [1]. To allow for direct comparison with the experimental results, the CFD model was setup to match the key characteristics of the experimental setup. The key characteristics are h_s/R, w/R, and the percentage of the cylinder cross-sectional area that is blocked by the baffle, where h_s is the height of the liquid above the baffle, R is the radius of the tank, and w is the wave height. Fig. 14 shows the geometry used in this paper, including the liquid fill level.

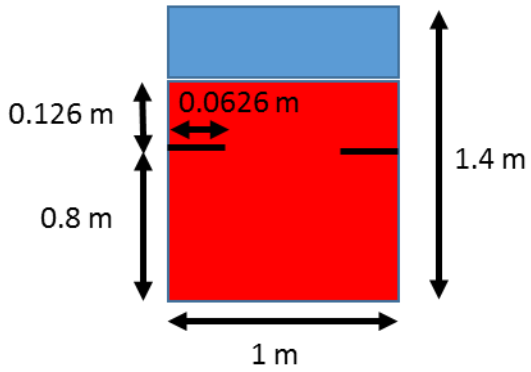

Figure 14. Cylindrical tank with ring baffle (not to scale)

Tab. 4 shows the mesh types, approximate cell count, and settling acceleration for the baffled tank cases.

Table 4. Ring Baffled tank model mesh type, cell count, and settling acceleration

Mesh Type	Approximate Cell Count	Settling Acceleration (m/s^2)
Polyhedral	390k	0.1
Polyhedral	637k	0.1
Polyhedral	1600k	0.1
Trim	564k	0.1

As explained in Section 2.1, the polyhedral mesh has been used extensively at GSFC because the main slosh plane is not known a priori. The trim mesh is included for completeness. Fig. 15 and Fig. 16 show cross-sections of the polyhedral mesh with approximately 637k cells and the trim mesh with approximately 564k cells.

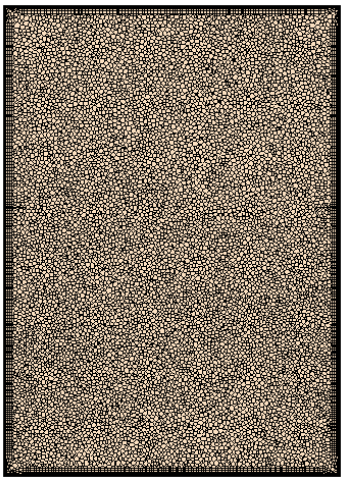

Figure 15. Polyhedral mesh with approximately 1600k cells

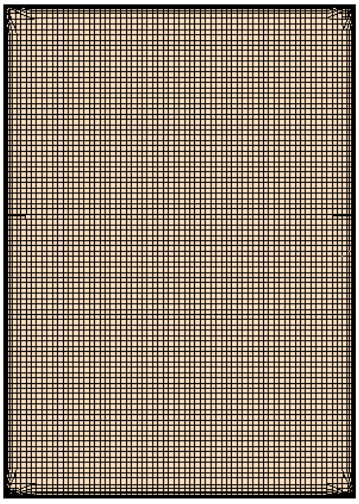

Figure 16. Trim mesh with approximately 564k cells

Unlike with the bare tank, no effort was made to refine the mesh near the liquid interface or near the baffles. Future research should include more mesh refinement near the liquid-gas interface and the baffles.

The model is initialized at a 10 degree angle to horizontal at a fill fraction of 0.126 m above the baffles. Fig. 17 shows the initialized state.

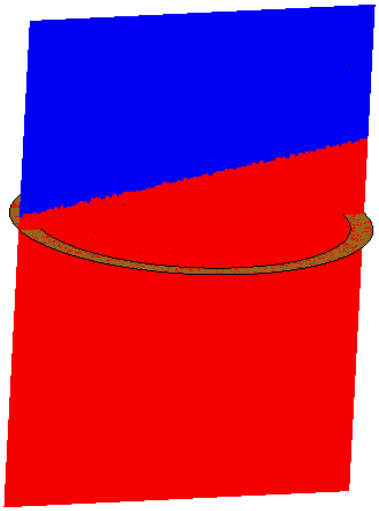

Figure 17. Initial conditions for ring baffled cylindrical tank models (bottom section is liquid)

By using a larger liquid offset angle than the bare tank, the effect of the wave height can be seen in the results.

As with the bare tanks, the liquid modeled is NTO and the gas modeled is nitrogen.

2.2.2 CFD results and discussion

The CFD model outputs for the ring baffled tank models are the same as those for the bare tank models. Fig. 18 and Fig. 19 show the center of mass and force plots for all of the different models. The models were run long enough to model at least 150 seconds of slosh. 150 seconds is enough time to see the damping trend. The results are truncated in the plots below to 75 seconds to better illustrate differences between the results. The CFD models output the torque, as with the bare tank model, but are not included in this paper because the behavior is similar to that of force.

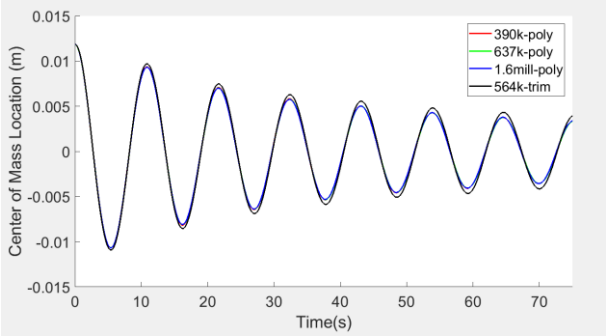

Figure 18. Center of mass movement for ring baffle tank models

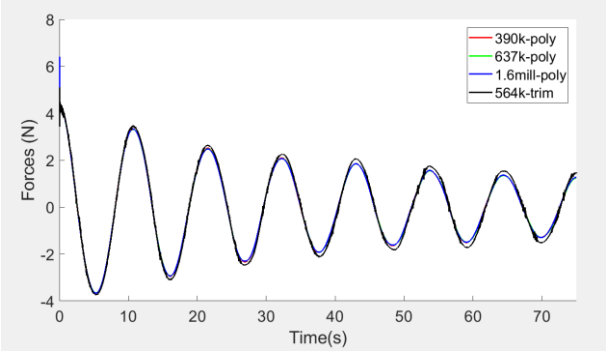

Figure 19. Forces on tank and baffle from ring baffle tank models

The results between the different polyhedral meshes are almost identical, but the trim mesh results in a lower damping than the polyhedral mesh. This behavior was also seen in the bare tank models. Fig. 20-22 show the force plot zoomed in over a range of times to better show the differences in the different models.

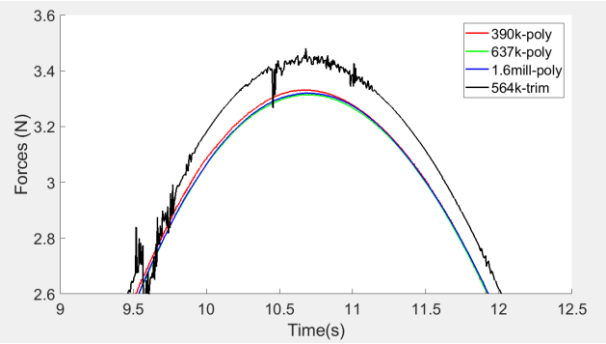

Figure 20. Forces from ring baffle tank models around 10.5 seconds (2nd peak)

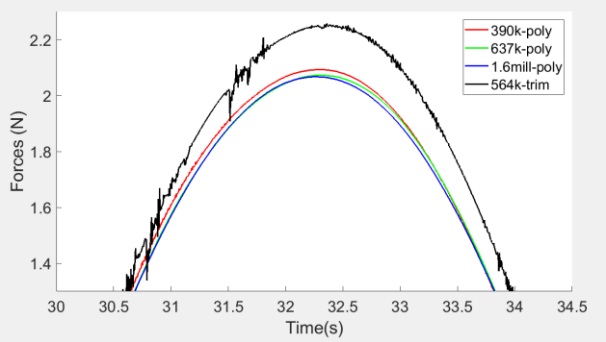

Figure 21. Forces from ring baffle tank models around 32.5 seconds (4th peak)

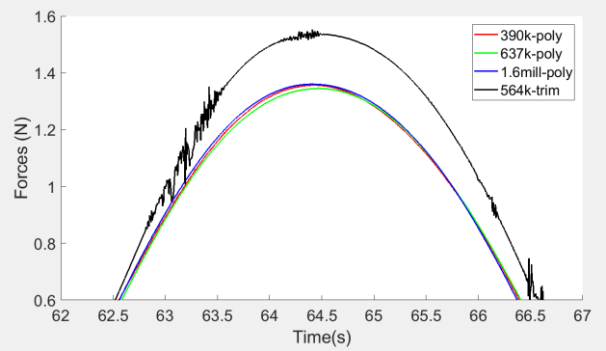

Figure 22. Forces from ring baffle tank models around 64.5 seconds (7th peak)

As with the bare tank models, the trim mesh force results show more noise than the polyhedral meshes. The noise is due to the model with the trim mesh not converging fully at each time step. The noise increases and decreases depending on how well the model is converging at a specific time step. The noise seen in the Fig. 20-22 is not seen when looking at the center of mass movement plots, but it is expected that the noise does contribute to errors in the center of mass movement plots.

Fig. 20-22 also show that the model results are similar for all the models with polyhedral meshes, regardless of mesh size. The model with the trim mesh gives force results that are consistently higher than the force results for the models with polyhedral meshes. The large difference between the damping at the beginning of the model runs for the model with a trim mesh and the models with a polyhedral mesh, indicate that an initial large difference in damping is carried throughout the model run. The results are similar between the polyhedral meshes because there is no model with a polyhedral mesh that has consistently higher or lower damping. The results from the different models with a polyhedral mesh are not converging or diverging over time.

The liquid-gas interface is well-defined during the sloshing model run, as shown in Fig. 23 and Fig 24.

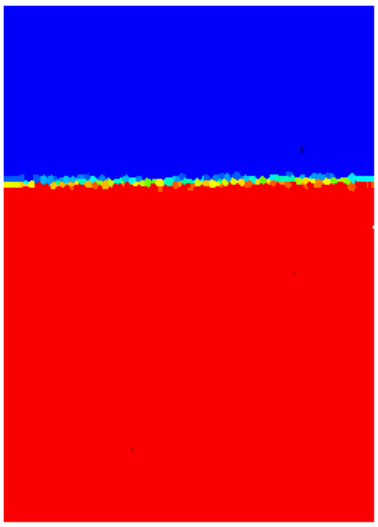

Figure 23. 390k polyhedral mesh liquid volume fraction (bottom section is liquid)

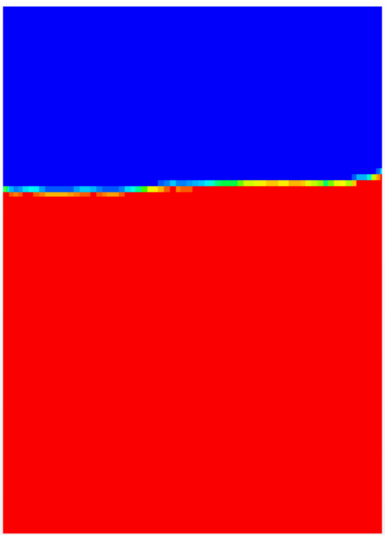

Figure 24. 564k polyhedral mesh liquid volume fraction (bottom section is liquid)

2.2.3 Post-processed CFD results and discussion

As with the bare tank, the frequency and damping ratios are calculated from the center of mass plots.

Because the damping due to the baffles is small, we expect the frequencies from the CFD to be approximately that of the slosh frequencies in a bare tank. The approach for calculating the frequency from the CFD data and the predicted tank frequency is the same as that for the bare tank. Eq. 8 is used to show how small the effects of damping are on the frequency, where f_d is the damped frequency and f_n is the undamped frequency. Because the damping in the ring baffle tank is changing over time, a damping ratio of 2%, or 0.02, is assumed when using Eq. 8 [9]. A choice of 3% or 4% damping would not change the results significantly.

$$f_d = f_n\sqrt{1-\zeta^2} \tag{8}$$

Tab. 5 shows a comparison between the frequency calculated from the CFD, the predicted frequency for a bare tank, and the predicted bare tank frequency when damping is considered. The extra digit is added to the bare tank and bare tank with damping frequencies to show that including damping does change the answer slightly.

Table 5. Ring baffled tank frequency comparison

Mesh Type	Frequency CFD (Hz)	Bare Tank Frequency Predicted (Hz)	Bare Tank With Damping Frequency (Hz)
390k	0.0935	0.09647	0.09645
637k	0.0934	0.09647	0.09645
1600k	0.0934	0.09647	0.09645
564k	0.0931	0.09647	0.09645

Unlike the bare tank models, the ring baffle tank CFD models give frequencies lower than expected, even when damping is considered. Using Eq. 8, it would take a damping ratio of about 25% before the bare tank frequency, adjusted for damping, would match the CFD frequency for the trim mesh. The differences in frequency are persistent with all models, but without further data, no conclusions can be made about the accuracy of the CFD frequency because it may be that the ring baffle is affecting the frequency more than just the damping implies.

The percent difference between the predicted frequency with damping considered and the frequency from the CFD model with the finest mesh is 3.2% and difference between the predicted frequency with damping and the frequency from the CFD model with a trim mesh is 3.4%. Depending on the application this level of accuracy may be sufficient.

Eq. 9 [10] and Eq. 10 [10] detail the logarithmic method for determining the damping ratio from the center of mass, where δ is the logarithmic decrement, x is the peak number in Fig. 25 or the equivalent figure for other models, and CM is the center of mass value of the peak referenced by the subscript x.

$$\delta = \frac{1}{0.5}\ln\frac{CM_x}{CM_{x+1}} \tag{9}$$

$$\zeta = \frac{1}{\sqrt{1+\left(\frac{2\pi}{\delta}\right)^2}} \tag{10}$$

To get a more accurate damping at a specific wave height, the negative peaks (referred to as valleys) are made into positive peaks, as shown in Fig. 25, by taking the absolute value of the center of mass CFD results.

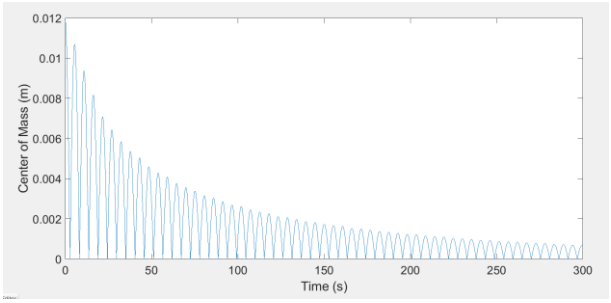

Figure 25. Center of mass plot for 390k model with absolute value of valleys

As with the bare tank, Eq. 7 was used to get a damping ratio that takes into account the frequency. E_{fit} is the logarithmic decrement damping instead of the exponential fit damping. The frequency from the CFD data was used in Eq. 7.

The wave height is back-calculated from the CFD model center of mass using the equation for the centroid of a cylindrical section [11]. The center of mass is calculated from averaging the peaks shown in Fig. 25 which are used in Eq. 7.

Fig. 26 shows the experimental results as taken from Fig. 2.7 in [1]. Because there is a lot of scatter in the damping calculated from the CFD results, a

logarithmic fit was calculated to better see the trend in the CFD data. The CFD model cylinder and baffle geometry were chosen to mimic an h_s/R of 0.252 and a baffle blockage of the cross-sectional area of the tank of 23.5%. These numbers were chosen to allow direct comparison with the results in Fig. 2.7 in [1].

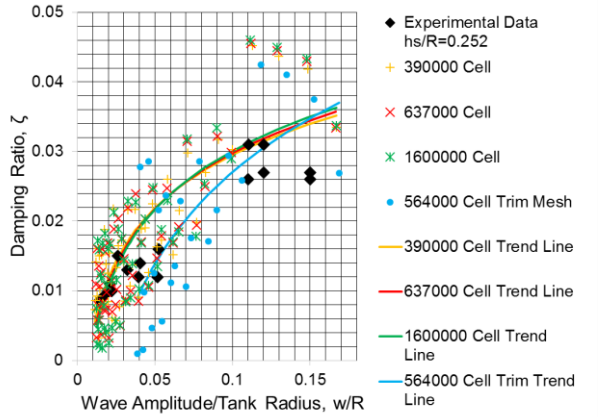

Figure 26. Comparison of ring baffle experimental damping results in black [1], and the CFD damping results for h_s/R =0.252 in color

Fig. 26 shows that regardless of mesh refinement, the models with polyhedral meshes give very similar results, but the model with a trim mesh gives lower damping values.

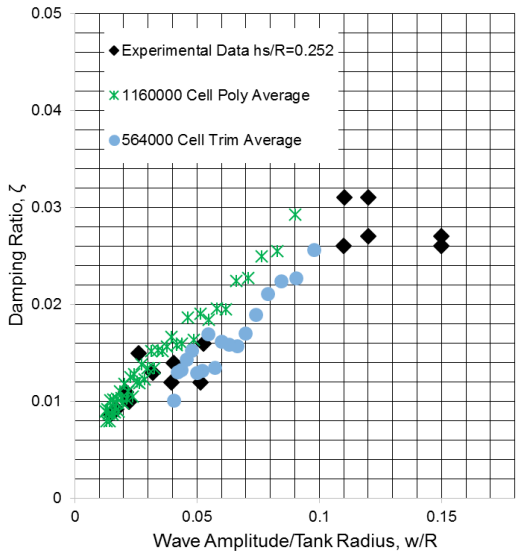

Figure 27. Comparison of ring baffle experimental damping results in black [1], and the CFD damping results for h_s/R =0.252 with 3 point moving average in color

Fig. 27 shows the results from the model with the finest polyhedral mesh and the results from the model with a trim mesh after further post-processing. This post-processing involves omitting the first 4 peaks to ensure that the transition from a flat liquid-gas interface to a wave shaped liquid-gas interface has occurred. Omission of the first few peaks is suggested by [7]. A 3 point moving average is taken of the remaining w/R and damping ratio values. The models with rougher polyhedral meshes are not plotted on Fig. 27 to increase the readability of the plot, but as shown in Fig. 26, the results from the models that are left out would match closely the results from the model with the finest polyhedral mesh.

The damping from the models with polyhedral meshes and the model with the trim mesh show good qualitative agreement with the experimental data when the first 4 peaks are thrown out and the 3 point moving average is done. The damping ratio from the models with polyhedral meshes is slightly higher than the average from the experimental data and the models with a trim mesh have damping that is slightly lower than the experimental data at low wave amplitudes. The differences can be attributed to the natural scatter in the data, experimental uncertainty, and error in the CFD model results.

The CFD results are used in NASA missions to create an equivalent mechanical model of the slosh with constant damping rather than a model with damping as a function of wave height. An exponential fit is made to the center of mass peak data to see how well constant damping matches the CFD results. The results are shown in Fig. 28.

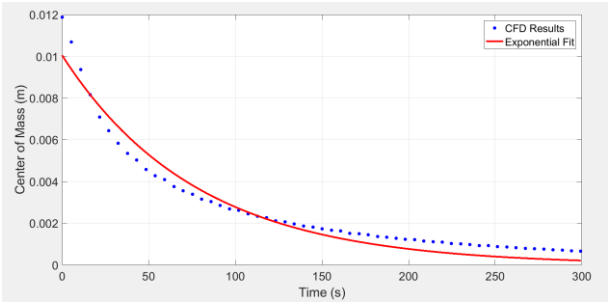

Figure 28. Exponential fit to CFD center of mass movement results for 390k model

The damping ratio calculated from the exponential fit in Fig. 28 is 0.0233 and the initial center of mass offset for the exponential fit is approximately 0.01. The initial center of mass offset for the CFD model is 0.012.

The results indicate that STAR-CCM+ can model the slosh frequency to within 3.2% and that the damping ratio values follow the experimental and

analytically derived trends in [1] with the magnitude of the damping ratio being good once the first few slosh cycles have occurred.

3. CONCLUSIONS

STAR-CCM+ CFD models of both a bare right cylindrical tank and right cylindrical tank with a ring baffle were studied. The mesh types, mesh cell counts, and local mesh refinement were varied to study how well STAR-CCM+ can model propellant slosh.

The CFD model with the finest polyhedral mesh matches the predicted frequency with a percent difference of 0.1% and matches the damping from the empirical correlations within a percent difference of 1.7% and 0.2%, respectively. The other models predict the frequency with a similar level of accuracy. The models with less refined polyhedral meshes over-predict the damping and the models with trim meshes under-predict the damping, when compared with the empirical correlations.

The CFD models of the ring baffled tank provided results that did not match the expected frequencies as well as the bare tank CFD models, but the model with the finest polyhedral mesh does match the predicted frequency, when damping is considered, with a difference of 3.2%. All of the ring baffled tank models predicted frequencies with similar level of accuracy. Both the models with a polyhedral mesh and the model with a trim mesh showed damping at each wave level that were above and below the expected damping. When a 3 point moving average is taken and the first 4 damping ratio values are thrown out, both models show good agreement with the experimental data, with models using the polyhedral mesh having the least difference with the experimental results. The results at the higher wave heights were harder to interpret, but the first peak under-predicted what was expected and the next 3 peaks over-predicted the expected damping.

The work in this paper shows that STAR-CCM+ gives valid results for both bare tanks and tanks with a single baffle. A model with a polyhedral mesh with an appropriate mesh refinement will give the best results.

4. ACKNOWLEDGMENTS

We would like to thank NASA's Europa Clipper project for funding this work.

5. REFERENCES

1. Dodge, F. T. (2000). *The New "Dynamic Behavior of Liquids In Moving Containers".* San Antonio, TX: Southwest Research Institute.

2. Ng, W., & Benson, D. (2017). Two-Pendulum Model of Propellant Slosh in Europa Clipper PMD Tank. *Thermal and Analysis Workshop 2017.* Huntsville, AL: NASA.

3. Benson, D. (2017). *Slosh Pendulum Parameter Summary Report (EUROPA-PROP-ANYS-0007 Rev B).* Greenbelt, MD: NASA.

4. Marsell, B. (2013). Experimental Validaiton of STAR-CCM+ For Liquid Container Slosh Dynamics. *STAR Global Conference 2013.*

5. Benson, D. J., & Mason, P. A. (2011). Method for CFD Simulation of Propellant Slosh in a Spherical Tank. *47th AIAA/ASME/SAE/ASEE Joint Propulsion Conference and Exhibit.* San Diego, CA: AIAA.

6. Musgrove, G., & Coogan, S. (2015). Validation and Rules-of-Thumb for Computational Predictions of Liquid Slosh Dynamics. *51st AIAA/SAE/ASEE Joint Propulsion Conference.* Orlando, FL: AIAA.

7. Yang, H., Purandare, R., Peugot, J., & West, J. (2012). Prediction of Liquid Slosh Damping Using a High Resolution CFD Tool. *48th AIAA/ASME/SAE/ASEE Joint Propulsion Conference.* Atlanta, GA: AIAA.

8. Siemens. (2017). *STAR-CCM+ 12.04.0.10-R8 Help Document.*

9. *Harmonic oscillator*. (2018, January 13). Retrieved from Wikipedia: https://en.wikipedia.org/wiki/Harmonic_oscillator

10. *Logarithmic decrement*. (2017, September 30). Retrieved from Wikipedia: https://en.wikipedia.org/wiki/Logarithmic_decrement

11. Cylindric Section. (2018, February 23). Retrieved from WolframMathWorld: http://mathworld.wolfram.com/CylindricSection.html